Band Structure of Graphite*

J. C. SLONCZEWSKI† AND P. R. WEISS
Rutgers, The State University, New Brunswick, New Jersey
(Received August 13, 1957)

Tight-binding calculations, using a two-dimensional model of the graphite lattice, lead to a point of contact of valence and conduction bands at the corner of the reduced Brillouin zone. A perturbation calculation which starts with wave functions of the two-dimensional lattice and is applied to the three-dimensional lattice is described. Some general features of the structure of the π bands in the neighborhood of the zone edge are obtained and are expressed in terms of appropriate parameters.

I. INTRODUCTION

SEVERAL attempts[1–3] have been made to explain the electrical and magnetic properties of graphite by a band structure based on a two-dimensional model of the lattice. This is reasonable in view of the physical structure of graphite; a layer lattice in which the separation of the layers is 3.35 A whereas the separation of atoms within a layer is 1.42 A. Moreover, the large anisotropies of the electrical conductivities and magnetic susceptibilities in and perpendicular to the basal planes make the two-dimensional model appear as an adequate approximation. Tight-binding calculations with this model lead to a contact of the valence and conduction bands at the corners of the Brillouin zone; the bands at the contact points have the form of circular cones in the space of energy *versus* wave number. This structure asserts that graphite behaves as a semiconductor with a vanishing energy gap, and in order to account for the electrical and magnetic properties it is necessary to invoke impurities or surface electrons.[4] A more telling difficulty is that the model does not allow for the presence of holes with different effective masses from the electrons.[5] The nature of the bands in the three-dimensional lattice is therefore of interest and the purpose of this paper is to display possible structures of the bands in the neighborhood of the edges, parallel to the c axis of the hexagonal Brillouin zone. The calculations are made by a perturbation calculation in which the zero-order wave functions are appropriate to layers of the lattice at the point of contact in the two-dimensional zone. The group theory of the two-dimensional lattice and the nature of the contact point are described in Sec. 2. The wave functions of the three-dimensional lattice and the appropriate perturbation calculation are described in Sec. 3 and the results are discussed in Sec. 4.

* This work has been partly supported by the Office of Naval Research and by the Rutgers University Research Council.
† Present address: International Business Machines Research Laboratory, Poughkeepsie, New York.
[1] P. R. Wallace, Phys. Rev. **71**, 622 (1947); **72**, 258 (1947).
[2] J. E. Hove, Phys. Rev. **100**, 645 (1955).
[3] J. W. McClure, Phys. Rev. **104**, 666 (1956).
[4] R. R. Hearing and P. R. Wallace, submitted to *Phys. and Chem. Solids*. We are indebted to the authors for permitting us to read this paper before publication.
[5] Galt, Yager, and Dail, Phys. Rev. **103**, 1586 (1956).

2. TWO-DIMENSIONAL LATTICE

Although the main purpose of the following calculations is an investigation of the three-dimensional lattice, we describe here the symmetry properties of the wave functions of a single layer, since these are used in the following section. Lomer[6] has presented a complete group-theoretical treatment of the single-layer lattice but this can be simplified greatly by a different choice of the location of the origin.

The two-dimensional lattice of carbon atoms is shown in Fig. 1. A unit cell, indicated by dashed lines, contains two atoms, one of type A and one of type B. The vectors $\mathbf{t}_1$ and $\mathbf{t}_2$ shown there are primitive translations ($\mathbf{t}_3=-\mathbf{t}_1-\mathbf{t}_2$). The length of each of these is a. The corresponding reciprocal lattice whose vectors are $\mathbf{K}_1$ and $\mathbf{K}_2$ is shown in Fig. 2. $\mathbf{K}_1$ and $\mathbf{K}_2$ satisfy the conditions,

$$\mathbf{K}_i\cdot\mathbf{t}_j=2\pi\delta_{ij};\quad i,j=1,2. \tag{2.1}$$

The points of contact are at U and U', the corners of the symmetrical reduced Brillouin zone which is indicated by the dashed lines of Fig. 2. The alternative zone indicated by solid lines is more convenient since it contains U and U' within it.

The calculations of Wallace[1] using tight-binding with π orbitals show that the contact points of the bands occur at U and U'. Numerical calculations made by

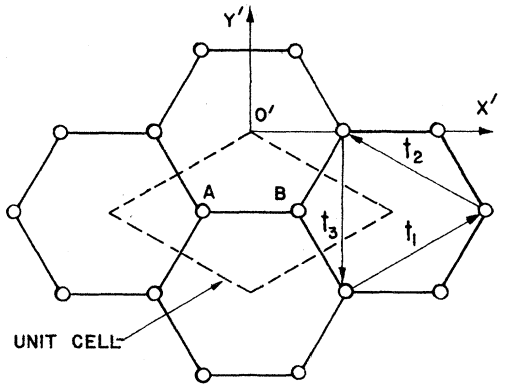

FIG. 1. A layer plane of the graphite lattice. The circles represent carbon atoms.

[6] W. H. Lomer, Proc. Roy. Soc. (London) **A227**, 330 (1955).

Corbato[7] show that the energy of the σ states are well removed from E^0, the energy at the points of contacts of the valence and conduction bands. It is reasonably certain, then, that the Fermi energy lies in the π bands and the discussion can be restricted to the symmetry properties of the π states.

Choosing the center of symmetry to be the origin of the coordinate axes shown in Fig. 1, permits a factorization of the space group into a point subgroup and the translation subgroup. The latter requires the wave function to satisfy the Bloch condition

$$\psi(\mathbf{k}, \mathbf{r}-\mathbf{t})=\exp(-i\mathbf{k}\cdot\mathbf{t})\psi(\mathbf{k},\mathbf{r}), \tag{2.2}$$

with

$$\mathbf{t}=n_1\mathbf{t}_1+n_2\mathbf{t}_2; \tag{2.3}$$

n_1 and n_2 are integers. A subgroup consisting of the identity element E and reflections in the plane (x,y), P_z can be factored from the point subgroup. This imposes the conditions

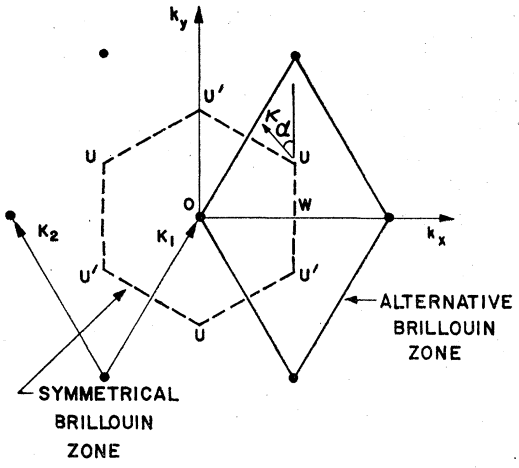

FIG. 2. The reciprocal lattice of the two-dimensional model. Two possible forms of the reduced Brillouin zone are shown.

$$P_z\psi(\mathbf{k},\mathbf{r})=+\psi(\mathbf{k},\mathbf{r}) \quad (\sigma \text{ states}), \tag{2.4}$$

$$P_z\psi(\mathbf{k},\mathbf{r})=-\psi(\mathbf{k},\mathbf{r}) \quad (\pi \text{ states}). \tag{2.5}$$

There remains only the subgroup of two-dimensional point group operations in the (x,y) plane. The plane group, $G(U)$, of the wave vector $\mathbf{k}_U$ is given in Table I. The characters of its irreducible representations U_i are listed in Table II.

The branching point energy, E^0, is fourfold degenerate as shown by Lomer[6] and by Carter.[8] Two of these states are at the point U and transform according to U_3 and two are at U' and transform isomorphically to U_3.

[7] F. J. Corbato, Ph.D. thesis, Massachusetts Institute of Technology, 1956 (unpublished).
[8] J. L. Carter, thesis, Cornell University, 1953 (unpublished).

TABLE I. Plane group, $G(U)$.

Elements	Description
E	identity
Q, Q^{-1}	rotation about z axis by $\pm\frac{2}{3}\pi$
T_1, T_2, T_3	reflections in (z,t_i) planes; $i=1, 2, 3$.

An explicit matrix representation for U_3 is

$$E=\begin{pmatrix}1&0\\0&1\end{pmatrix},\quad Q=\begin{pmatrix}\omega^{-1}&0\\0&\omega\end{pmatrix},\quad Q^{-1}=\begin{pmatrix}\omega&0\\0&\omega^{-1}\end{pmatrix},$$

$$T_1=\begin{pmatrix}0&\omega\\\omega^{-1}&0\end{pmatrix},\quad T_2=\begin{pmatrix}0&\omega^{-1}\\\omega&0\end{pmatrix},\quad T_3=\begin{pmatrix}0&1\\1&0\end{pmatrix},$$

$$\omega=e^{\frac{2}{3}\pi i}. \tag{2.6}$$

A knowledge of the transformation properties of the wave functions belonging to U_3, u_{31}, and u_{32}, at the point $\mathbf{k}_U=\mathbf{k}_0$ makes it possible to determine the energy $E(\mathbf{k})$ in the neighborhood of $\mathbf{k}=\mathbf{k}_0$. The Bloch wave functions $\psi(\mathbf{k},\mathbf{r})$ satisfy

$$\left(-\frac{\hbar^2}{2m}\nabla^2+V(\mathbf{r})-E(\mathbf{k})\right)\psi(\mathbf{k},\mathbf{r})=0. \tag{2.7}$$

The Bloch function having the wave vector $\mathbf{k}_0+\boldsymbol{\kappa}$ can be written as

$$\psi(\mathbf{k}_0+\boldsymbol{\kappa}, \mathbf{r})=\exp(i\boldsymbol{\kappa}\cdot\mathbf{r})\phi(\mathbf{k}_0,\mathbf{r}), \tag{2.8}$$

where $\phi(\mathbf{k}_0,\mathbf{r})$ obeys the Bloch condition (2.2). On substituting this into (2.7), one finds

$$\left(-\frac{\hbar^2}{2m}\nabla^2+V(\mathbf{r})+H'-E(\mathbf{k}_0+\boldsymbol{\kappa})\right)\phi(\mathbf{k}_0,\mathbf{r})=0, \tag{2.9}$$

with

$$H'=(\hbar/m)\boldsymbol{\kappa}\cdot\mathbf{p}+\hbar^2\kappa^2/2m. \tag{2.10}$$

The operator H' is invariant with respect to lattice translations and therefore connects only states of the same $\mathbf{k}$. The problem of determining $E(\mathbf{k}_0+\boldsymbol{\kappa})$ is therefore reduced to finding the energy change induced on $E(\mathbf{k}_0)$ by the perturbation energy H'; the unperturbed energy $E^0=E(\mathbf{k}_0)$ is doubly degenerate with wave functions u_{31} and u_{32}.

It is convenient to set

$$\boldsymbol{\kappa}=(-\kappa\sin\alpha, \kappa\cos\alpha, 0), \tag{2.11}$$

TABLE II. Characters of the "small" representations U_i of $G(U)$.

Representation	ϵ	Class Q	T
U_1	1	1	1
U_2	1	1	−1
U_3	2	−1	0

with α shown in Fig. 2, and to define the operators $p(\alpha)$ by

$$p(\alpha)=\boldsymbol{\kappa}\cdot\mathbf{p}/\kappa=-p^x\sin\alpha+p^y\cos\alpha. \quad (2.12)$$

Then,

$$H'=(\hbar/m)\kappa p(\alpha)+\hbar^2\kappa^2/2m. \quad (2.13)$$

The operators

$$\pi^1=\frac{1}{\sqrt{2}}(p^x+ip^y) \quad \text{and} \quad \pi^2=\frac{1}{\sqrt{2}}(-p^x+ip^y) \quad (2.14)$$

transform under rotations of coordinate axes according to U_3. In terms of these operators,

$$p(\alpha)=\frac{-i}{\sqrt{2}}(\pi^2e^{i\alpha}+\pi^1e^{-i\alpha}). \quad (2.15)$$

The matrix elements of π^S $(S=1, 2)$ can be partially determined by using the transformation properties of the wave functions under the operations of the group elements. One finds

$$(u_{\mu\nu}\pi^S u_{ij})=\frac{1}{h}\sum_R\sum_{\nu'S'j'}{}^{\mu}D_{\nu'\nu}{}^*(R) \times{}^3D_{S'S}(R)\ {}^iD_{j'j}(R)\ (u_{\mu\nu'}\pi^{S'}u_{ij'}). \quad (2.16)$$

Here h is the number (6) of elements, R, in the group; ${}^iD_{j'j}(R)$ is the $(j'j)$ element in the matrix representative of the group element R in the ith representation. By performing the sums shown in (2.16) and using (2.6), Table II, and (2.15) one finds the submatrix of $p(\alpha)$ in u_{31} and u_{32} is

$$p(\alpha)=-p_0\begin{pmatrix}0 & e^{i\alpha}\\ e^{-i\alpha} & 0\end{pmatrix}, \quad (2.17)$$

where p_0 is a real constant. The reality of p_0 is a consequence of the Hermitian property of p^x and p^y. In addition to the elements shown in (2.17) there are also others which connect u_{31} with the one-dimensional states. Although these are not used in the present section they will be in the following one and are listed here.

$$\begin{aligned}p(\alpha)_{31;11}&=\beta e^{-i\alpha},\\ p(\alpha)_{32;11}&=\beta e^{+i\alpha},\\ p(\alpha)_{31;21}&=\gamma e^{-i\alpha},\\ p(\alpha)_{32;21}&=-\gamma e^{+i\alpha}.\end{aligned} \quad (2.18)$$

Here β and γ are constants not determined by the symmetry but by the explicit wave functions u_{ij}.

The result of diagonalizing the perturbation H', (2.13) leads to energy values which are, to first order in κ,

$$\begin{aligned}E_1(\mathbf{k}_0+\boldsymbol{\kappa})&=E^0-(\hbar p_0/m)\kappa,\\ E_2(\mathbf{k}_0+\boldsymbol{\kappa})&=E^0+(\hbar p_0/m)\kappa.\end{aligned} \quad (2.19)$$

The energy surface is a circular cone to first order in κ, in E, κ_x, κ_y space. This result is independent of any approximations regarding wave functions and is a result of the symmetry of an isolated graphite layer with spin-orbit coupling neglected. The tight-binding calculations agree with (2.19) in the limit of small κ.

TABLE III. Numerical values of $p_0/\hbar$ in A^{-1}.

$p_0/\hbar$	Source
0.25	Wallace[a]
0.80	Lomer[b]
0.63	present authors
0.72	McClure[c]

[a] See reference 1.
[b] See reference 6.
[c] See reference 3.

The parameter p_0 can be determined only with the use of explicit wave functions. In terms of Wallace's overlap integral γ_0, it is

$$p_0=(\tfrac{3}{2})^{\frac{1}{2}}a(m/\hbar)\gamma_0, \quad (2.20)$$

where a is a lattice parameter, 2.456 A.[9] Coulson, according to Wallace, estimates γ_0 to be 0.9 ev whereas Lomer,[6] using atomic wave functions in a tight-binding calculation, estimates it to be 3 ev. The corresponding values of p_0 are shown in Table III. In the appendix we estimate p_0 by assuming that u_{31} and u_{32} can be written as Bloch sums of hydrogenic orbitals. McClure's[3] value was obtained by a comparison of calculated values of magnetic susceptibility at high temperatures with experiment and so is derived from experiment. Our value agrees favorably with this.

The algebraic sign of p_0 is of interest for if p_0 is negative, the valence band must overlap the conduction band.[10] The argument for this is based on the compatibility relations of the small representations[11] and on the argument that the algebraic sign of at least one of the four π-band energy differences is given correctly by the tight-binding method. However, it is to be noticed that p_0 is positive.

The effect of spin-orbit coupling on the energy levels deserves brief mention. Using the methods described by Elliot,[12] it is found that spin-orbit coupling separates the energies E^0. However, this requires an admixture of atomic states with principal quantum number greater than two. This fact combined with the small nuclear charge of carbon causes the splitting to be less than 10^{-4} ev. The details of this calculation are given in reference 10.

3. THREE-DIMENSIONAL LATTICE

The three-dimensional lattice has a 180° screw axis perpendicular to the basal plane. Similar layers are

[9] W. Trzebiatowski, Roczniki Chem. **17**, 73 (1937) [see Chem. Abstr. **31**, 4177 (1936)].
[10] J. Slonczewski, thesis, Rutgers University, 1955 (unpublished). Mic. 56–2314. Microfilm or photostatic copies available from University Microfilms, Ann Arbor, Michigan, 1956.
[11] Bouckaert, Smoluchowski, and Wigner, Phys. Rev. **50**, 58 (1936).
[12] R. J. Elliot, Phys. Rev. **96**, 280 (1954).

stacked with corresponding A and B atoms above each other a distance c apart; these layers are numbered $1, 3, 5\cdots$. Half-way between these layers are layers with A' atoms above A atoms but because of the rotation about the screw axis, the B' atoms do not lie in line with the B atoms; these layers are numbered $2, 4, 6, \cdots$. A projection of the lattice onto a single plane illustrating this structure is shown in Fig. 3. A unit cell contains one of each of the four types of atoms, A, A', B, B'. The lattice translations are

$$\mathbf{t}=n_1\mathbf{t}_1+n_2\mathbf{t}_2+n_4\mathbf{t}_4,$$

where n_1, n_2, n_4 are integers. The vector $\mathbf{t}_4$ has a magnitude c and is directed parallel to the z axis, perpendicular to the planes.

Two forms of the reduced Brillouin zone are shown in Fig. 4. Each is a prism derived from the corresponding zone of the two-dimensional lattice. The dashed

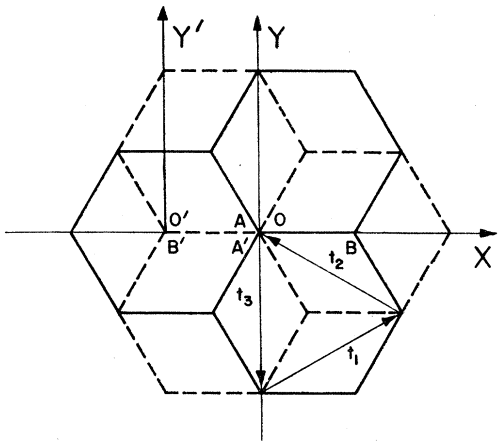

FIG. 3. A projection of the graphite lattice on a layer plane. The solid (dashed) lines join the projections of atoms of types A and B (A' and B') in odd (even) numbered layers.

lines show the usual zone having sixfold symmetry about the k_z axis. If the layers were separated to infinity, the states with wave vectors lying on the lines HH and $H'H'$ would reduce to those having wave vectors U and U', respectively. It is those states which lie near the edges HH and $H'H'$ which are of primary interest and, accordingly, the alternative zone represented by solid lines is more convenient. A general point on the edge HH is denoted by S.

A group-theoretical analysis of the three-dimensional lattice has been carried out by Carter[8] ‡ and we use his results to obtain the wave functions. The group of the wave vectors $\mathbf{k}_s$, $G(S)$, and its representations are shown in Table IV. This is abridged in that the translations are not shown explicitly. The translation $\mathbf{t}_4/2$ cannot be factored from $G(S)$. It is to be noticed that the origin here is at an A atom whereas the center of symmetry for the layer functions u_1 and u_2 is at O'

‡ See also, C. Herring, J. Franklin Inst. 233, 525 (1942).

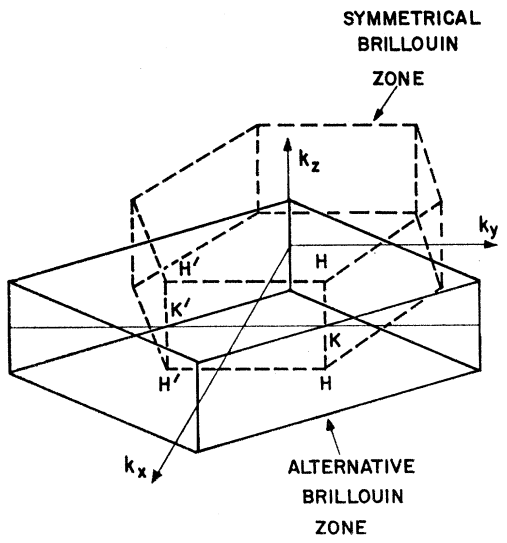

FIG. 4. Two possible forms of the three-dimensional reduced Brillouin zone.

shown in Fig. 3. The ρ_i used in Table IV is labeled ρ_i'' by Carter.

An explicit matrix representation of S_3 is

$$(\epsilon/0)=\begin{pmatrix}1&0\\0&1\end{pmatrix},\quad(\delta_3/0)=\begin{pmatrix}\omega^{-1}&0\\0&\omega\end{pmatrix},\quad(\delta_3^{-1}/0)=\begin{pmatrix}\omega&0\\0&\omega^{-1}\end{pmatrix},$$

$$(\rho_1/\tfrac{1}{2}\mathbf{t}_4)=\exp(-i\mathbf{k}_S\cdot\mathbf{t}_4/2)\begin{pmatrix}0&\omega\\\omega^{-1}&0\end{pmatrix},$$

$$(\rho_2/\tfrac{1}{2}\mathbf{t}_4)=\exp(-i\mathbf{k}_S\cdot\mathbf{t}_4/2)\begin{pmatrix}0&\omega^{-1}\\\omega&0\end{pmatrix},\tag{3.1}$$

$$(\rho_3/\tfrac{1}{2}\mathbf{t}_4)=\exp(-i\mathbf{k}_S\cdot\mathbf{t}_4/2)\begin{pmatrix}0&1\\1&0\end{pmatrix},\quad\omega=e^{\frac{2}{3}\pi i}.$$

In the three-dimensional lattice there are four atoms per unit cell, twice as many as in the layer model. Each layer state must give rise to two three-dimensional states at each $\mathbf{k}$. Each of the layer π states, $u_{31}=u_1$ and $u_{32}=u_2$, give two ψ's at $\mathbf{k}_S$. These ψ's transform according to the representations in Table IV and are labeled

TABLE IV. The group $G(S)$ and its small representations.

Operator		Definition	
ϵ		identity	
δ_3, δ_3^{-1}		rotations by $\pm\frac{2}{3}\pi$ about z axis	
ρ_1, ρ_2, ρ_3		reflections in (t_4t_i) planes; $i=1, 2, 3$	
Representation	$(\epsilon/0)$	Group elements $(\delta_3/0)$, $(\delta_3^{-1}/0)$	$(\rho_1/\frac{1}{2}\mathbf{t}_4)$
S_1	1	1	$\exp(-i\mathbf{k}_S\cdot\mathbf{t}_4/2)$
S_1	1	1	$-\exp(-i\mathbf{k}_S\cdot\mathbf{t}_4/2)$
S_3	2	-1	0

ψ_{11}, ψ_{21}, ψ_{31}, and ψ_{32}. They are

$$\psi_{31}=b'=\sum_s e^{ick_z(s+\frac{1}{2})}(\rho_3/(s+\tfrac{1}{2})\mathbf{t}_4)u_1, \tag{3.2}$$

$$\psi_{32}=b=\sum_s e^{ick_z s}(\epsilon/s\mathbf{t}_4)u_1, \tag{3.3}$$

$$\psi_{21}=\frac{1}{\sqrt{2}}(a-a'), \tag{3.4}$$

$$\psi_{11}=\frac{1}{\sqrt{2}}(a+a'), \tag{3.5}$$

with

$$a=\sum_s e^{ick_z s}(\epsilon/s\mathbf{t}_4)u_2, \tag{3.6}$$

$$a'=\sum_s e^{ick_z(s+\frac{1}{2})}(\rho_3/(s+\tfrac{1}{2})\mathbf{t}_4)u_2. \tag{3.7}$$

The notation is chosen to convey the nature of the ψ's. If the function a, for example, were written as a linear combination of atomic p_z orbitals, only those located on type-A atoms would occur. Analogous statements apply to a', b, b', and A', B, B', respectively. However, for our purposes it is not necessary to assume such an expansion. That the wave functions (3.2) to (3.7) transform properly can be verified readily in the usual way by noting that

$$\begin{aligned}
&(\delta_3/0)=(Q/-\mathbf{t}_2),\\
&(\delta_3^{-1}/0)=(Q^{-1}/\mathbf{t}_1),\\
&(\rho_1/0)=[T_1/-\tfrac{1}{3}(\mathbf{t}+2\mathbf{t}_2)],\\
&(\rho_2/0)=[T_2/\tfrac{1}{3}(2\mathbf{t}_1+\mathbf{t}_2)],\\
&(\rho_3/0)=[T_3/\tfrac{2}{3}(1\mathbf{t}_1-\mathbf{t}_2)][T_3/\tfrac{2}{3}(\mathbf{t}_1-\mathbf{t}_2)],
\end{aligned} \tag{3.8}$$

and that

$$\mathbf{k}_S=\tfrac{2}{3}\mathbf{K}_1-\tfrac{1}{3}\mathbf{K}_2+k_z\mathbf{e}_z, \tag{3.9}$$

where $\mathbf{e}_z$ is a unit vector in the z direction. The relations (3.8) arise from the different choices of centers of symmetry, that for the layer function and that used by Carter. They are written explicitly for the odd-numbered layers.

The wave functions (3.2) to (3.7) are only approximate since the layer functions u_1 and u_2 have π symmetry; they are correct in the limit where overlap energies between layers are negligible. For arbitrary values of k_z, other than $\pm\pi/c$ and 0, one should include layer functions of σ symmetry, as well as π symmetry. The amplitude of the σ component is of the order of the overlap energy between neighboring layer atoms using π and σ wave functions divided by the energy difference between π and σ states. This overlap energy is less than the overlap energy between A and A' atoms using π functions and this is to be divided by the large energy separation between π and σ states. We conclude that the ψ's, though approximate, are satisfactory wave functions.

The energies of the states (3.2) to (3.5) vary with k_z and will be denoted by $E_i^0(k_z)$, $i=1, 2, 3$ corresponding to the different representations. Possible forms of these variations are shown in Figs. 5 and 6. As Table IV shows, the energy for an arbitrary point S on HH consists of two single levels and one doubly degenerate one. As Carter's analysis shows, the two single levels coalesce at H, where $k_z=\pm\pi/c$, to the value $E_1(H)$. The symmetry of the lattice does not require this energy value to be the same as the value $E_3(H)$ of the doubly degenerate level.

We now calculate the energy in the neighborhood of the line HH using the method of Sec. II. We set $\mathbf{k}=\mathbf{k}_S+\boldsymbol{\kappa}$, with $\kappa_z=0$, and calculate $E(k_S+\kappa)$ by diagonalizing the perturbed Hamiltonian H_0+H' restricting the matrix of H to be the submatrix in the ψ_{lm}. The assumption here is that connections with other π states are negligibly small since they are far removed in energy. From the formal similarity between the small representations of k_S in the three-dimensional model and those of k_U in the two-dimensional model it follows that $p(\alpha)$ is represented by matrices of the same form in the corresponding manifolds. Using (2.13), (2.17), and (2.18) for the matrix elements of $p(\alpha)$ connecting different representations and also (3.4) and (3.5), the submatrix of H_0+H' in the orthogonal set b, a, a', b' is

$$\begin{array}{c} \\ b \\ a \\ a' \\ b' \end{array}\!\!\begin{array}{c} \begin{array}{cc} b & a \end{array} \\ \begin{pmatrix} E_3^0+F & -D(1+r) \\ -D^*(1+r^*) & \tfrac{1}{2}(E_1^0+E_2^0)+F \\ p^*D & \tfrac{1}{2}(E_1^0-E_2^0) \\ qD & pD^* \end{pmatrix} \end{array}\!\!\begin{array}{c} \begin{array}{cc} a' & b' \end{array} \\ \begin{pmatrix} pD & qD^* \\ \tfrac{1}{2}(E_1^0-E_2^0) & p^*D \\ \tfrac{1}{2}(E_1^0+E_2^0)+F & -D(1+r^*) \\ -D^*(1+r) & E_3^0+F \end{pmatrix} \end{array}. \tag{3.10}$$

Here $F=\hbar^2\kappa^2/2m$ and $D=(\hbar p_0/m)\kappa e^{i\alpha}$. The coefficients p, q, r, are functions of k_z which could be determined only from explicit wave functions. The elements containing p and q connect atoms B and A', B and B' and A and B', that is to say atoms on neighboring layers but not directly above each other as does the matrix element connecting a and a'. Such terms though not required by the symmetry to vanish are small. The particular element in q, though q is small, can be important since it connects degenerate states. We conclude that the elements in p and r can be omitted. We temporarily drop the element in q and return to it below. The resulting determinantal equation for the energy can be factored to

$$\begin{vmatrix} E_3^0+F-E & -(\hbar/m)p_{0\kappa} \\ -(\hbar/m)p_{0\kappa} & E_1^0+F-E \end{vmatrix}\begin{vmatrix} E_2^0+F-E & -(\hbar p_0/m)\kappa \\ -(\hbar p_0/m)\kappa & E_3^0+F-E \end{vmatrix}=0. \tag{3.11}$$

The solutions of (3.11) are

$$E_1, E_3=\tfrac{1}{2}(E_1^0+E_3^0)\pm[\tfrac{1}{4}(E_1^0-E_3^0)^2+(\hbar^2/m^2)p_0^2\kappa^2]^{\frac{1}{2}},$$
$$E_2, E_3^1=\tfrac{1}{2}(E_2^0+E_3^0)\pm[\tfrac{1}{4}(E_2^0-E_3^0)^2+(\hbar p_0/m)\kappa^2]^{\frac{1}{2}}. \quad (3.12)$$

The signs are chosen in such a way that $E_i(\kappa=0)=E_i^0$. The term F is neglected because it is of the same order of magnitude as terms resulting from connections to wave functions which have been neglected. The energy surfaces described by (3.12) represent the energy, therefore, only in a small neighborhood of the lines HH and $H'H'$. For constant k_z the energy surfaces in E, κ_x, κ_y space consist of four hyperbolas of revolution illustrated in Fig. 7. We observe that, depending on the order of $E_i^0(k_z)$, the valence and conduction bands touch [Fig. 6] or leave a gap [Fig. 5]. However, within a plane $k_z=$constant the bands do not overlap in the approximations we are considering.

The inclusion of the term in q connecting states b and b', but not the terms in p and r, leads to a complicated behavior of the energies. One finds, for $\alpha=0$

$$E_1, E_3=\tfrac{1}{2}(E_1^0+E_3^0+qD')\pm[\tfrac{1}{4}(E_1^0-E_3^0-qD')^2+D'^2]^{\frac{1}{2}}$$
$$E_2, E_3^1=\tfrac{1}{2}(E_2^0+E_3^0-qD')\pm[\tfrac{1}{4}(E_2^0-E_3^0+qD')^2+D'^2]^{\frac{1}{2}} \quad (3.13)$$

where $D'=(\hbar p_0/m)\kappa_y$. Here again the term F is neglected. A sketch of the variation of E_3 with κ is shown in Fig. 8 for $\kappa_x=0$. The figure has a threefold symmetry about the E axis. Such a behavior of the energy has been discussed by Johnston.[13]

4. DISCUSSION

In the previous section we derived the expressions (3.12) for $E_i(k_z)$ as functions of κ_x and κ_y. These may be used to determine the effective masses of electrons and holes in planes perpendicular to the z axis. They

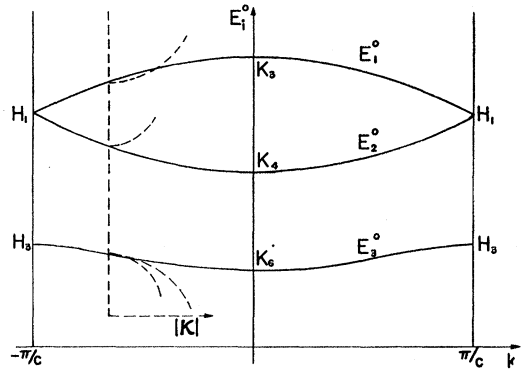

FIG. 5. The solid curves show a possible dependence of band energy on k_z along the c edge of the hexagonal zone. The dashed curves illustrate the dependence of energy on κ_x and κ_y for constant k_z. A gap separates the conduction and valence bands.

[13] D. F. Johnston, Atomic Energy Research Establishment, Harwell Report T/R-855, 1952 (unpublished); Proc. Roy. Soc. (London) **A227**, 349 and 359 (1955).

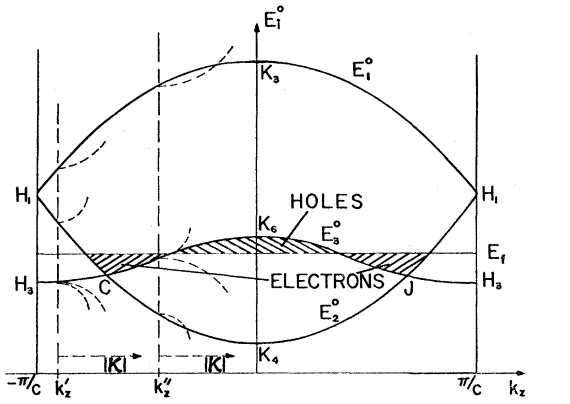

FIG. 6. Another possible version of Fig. 5. Here the conduction and valence bands overlap. E_f is the Fermi energy at absolute zero.

do, however, contain certain parameters which are difficult to determine from first principles but conceivably can be determined from experiment. These parameters are p_0 and those involved in the functions of k_z, $E_i^0(k_z)$. So far, only estimates have been made for the variations of E_i^0 with k_z, based on tight-binding approximations[1,6,13,14] though certain general statements can be made in the light of the wave functions (3.2) to (3.7). The functions u_1 and u_2 there can be viewed as layer analogs to Wannier functions.

1. In the tight-binding approximation, $\psi_{11}(H)$ and $\psi_{21}(H)$ are linear combinations of orbitals on A atoms and $\psi_{32}(H)$ and $\psi_{31}(H)$ are linear combinations of orbitals on B atoms. The fact that A and B atoms do not experience the same crystalline fields is responsible for the difference in the energies $E_3^0(H_1)$ and $E_1^0(H_1)$ [or $E_2^0(H_1)$]. The degeneracy of $E_1^0(H_1)$ and $E_2^0(H_1)$ at the point H_1 is a consequence of the symmetry of the crystal.

2. The overlap of the layer π functions on nearest neighbor layers is sufficient to cause $E_1^0(k_z)$ and $E_2^0(k_z)$ to depend upon k_z. If only such interactions are included the variation is

$$E_{1,2}(k_z)=E_1(H_1)\pm\delta_1\cos(ck_z/2). \quad (4.1)$$

3. The wave functions ψ_{31} and ψ_{32} as written in (3.2) and (3.4) are Bloch sums of layer functions on *alternate* layers. Therefore $E_3^0(k_z)$ depends on k_z only by virtue of overlaps between layers which are *second nearest* neighbors or more distant neighbors. The largest of these are presumably those that arise from second nearest neighbors and the resulting energy dependence on k_z has the form

$$E_3^0(k_z)=E_3^0(H_3)+\delta_2[1-\sin^2(\tfrac{1}{2}ck_z)]. \quad (4.2)$$

Since nearest neighbor effects, if not forbidden by symmetry, should be greater than more distant effects,

[14] J. L. Carter and J. A. Krumhansl, J. Chem. Phys. **21**, 2238 (1953); M. Yamazaki, J. Chem. Phys. **26**, 930 (1957).

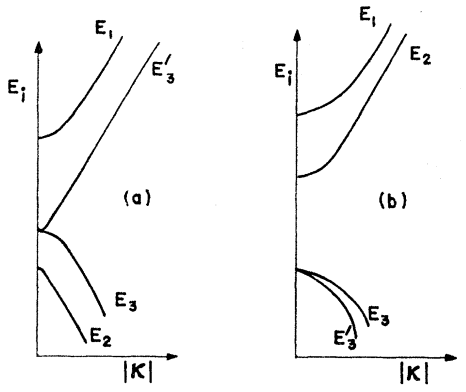

FIG. 7. Schematic dependence of band energy on κ for constant k_z, illustrating two possible cases.

we assume E_1^0 and E_2^0 to vary much more with k_z than E_3^0.

4. If the effect described in 1 is larger than that described in 2, there is a gap between valence and conduction bands, and this is illustrated in Fig. 5. If the reverse is true, a gap exists only in a small neighborhood of $k_z=\pm\pi/c$; beyond this there is a touching of the valence and conduction bands, as is illustrated in Fig. 6.

5. The form of the bands illustrated in Fig. 6 permit the possibility of the existence of free electrons and holes. The lowest valley of the conduction band runs along the broken curve $H_1CK_6JH_1$ and the highest ridge of the valence band runs along $H_3CK_6JH_3$. These facts are made apparent by noting the dashed curves of Fig. 6 which depict E_i^0 *versus* κ at typical values of k_z in accordance with Fig. 7. The position of the Fermi level at absolute zero is sketched in the same Fig. 6; one sees that this lies below the top of the valence band at the point K_6 and above the bottom of the conduction band at the points C and J. The relatively small variation of E_3 with k_z then accounts for the small number of electrons and holes and a consequent low value for the degeneracy temperature.

6. The variation of the energies with κ as given by (3.12) leads to effective masses for the electrons and holes which are variable with κ in the (x,y) plane.

7. The discussion above is based on the energies as described by (3.12). These omit the connection in energy between the degenerate states $E_3^0(k_z)$. When this is taken into account, the energies are modified and are described by (3.13). The behavior of the surfaces are shown in Fig. 8. The curve $WSXYZ$ lies in the conduction band and $RSTYV$ lies in the valence band. An overlap can occur since the point Y need not have the same energy as that of S. In addition, the rotational symmetry of the energy surface about the E axis of E, κ_x, κ_y, space is destroyed. This type of energy surface has been discussed by Johnston.[13] We have not been able to assess the importance of this effect.

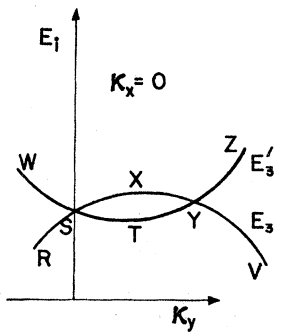

FIG. 8. A portion of Fig. 7(a) enlarged to illustrate the effect of a higher order approximation.

It is possible that the parameters which determine the energy bands of graphite may be determined empirically. Considerable progress in this direction has been made by McClure[15] through an analysis of the de Haas-van Alphen effect. He finds that bands of the form shown in Fig. 6 can explain this effect.

APPENDIX

In this appendix, the parameter p_0, defined in (2.17), is estimated by writing u_{31} and u_{32} as Bloch sums of hydrogenic orbitals. From Eqs. (2.12) and (2.17) it follows that the function

$$w_0=\frac{1}{\sqrt{2}}(u_{32}-u_{31}) \tag{a.1}$$

has the eigenvalue p_0 for p_y. Therefore,

$$p_0=\int w_0^*(\mathbf{r})p_y w_0(\mathbf{r})\mathbf{dr}. \tag{a.2}$$

One can write the Fourier series

$$w_0(\mathbf{r})=(1/2\pi)\textstyle\sum_\kappa c(\mathbf{k}_u+\mathbf{K},z)\exp[i(\mathbf{k}_u+\mathbf{K})\cdot\mathbf{r}], \tag{a.3}$$

with

$$c(\mathbf{k}_u+\mathbf{K},z)=\frac{2\pi}{\Omega}\int\int\exp[-i(\mathbf{k}_u+\mathbf{K})\cdot\mathbf{r}]w_0(\mathbf{r})dxdy,$$

the integration being taken over a two-dimensional unit cell of area Ω. The vector $\mathbf{K}$ is a reciprocal lattice vector,

$$\mathbf{K}=l_1\mathbf{K}_1+l_2\mathbf{K}_2. \tag{a.4}$$

Then,

$$p_0=\hbar\sum_\kappa(\mathbf{k}_u+\mathbf{K})_y\int_{-\infty}^{+\infty}|c(\mathbf{k}_u+\mathbf{K},z)|^2dz.$$

The representation displayed in (2.6) requires the following form of w_0 when written as a Bloch sum of atomic $2p_z$ orbitals represented by $f(\mathbf{r})$:

$$w_0(\mathbf{r})\sim\sum_{\mathbf{t}}\exp(i\mathbf{k}_u\cdot\mathbf{t})[f(\mathbf{r}-\mathbf{t}_A-\mathbf{t})-f(\mathbf{r}-\mathbf{t}_B-\mathbf{t})]. \tag{a.5}$$

[15] J. W. McClure, Phys. Rev. **108**, 612 (1957). We are indebted to Dr. McClure for a discussion of his work prior to publication.

The summation is carried over the two-dimensional lattice. The Fourier coefficients are proportional to

$$c(\mathbf{k}_u+\mathbf{K}, z)\sim\sum_{\mathbf{t}}\int_{\Omega}\int \exp[-i(\mathbf{k}_u+\mathbf{K})\cdot(\mathbf{r}-\mathbf{t})] \times[f(\mathbf{r}-\mathbf{t}_A)-f(\mathbf{r}-\mathbf{t}_B)]dxdy \quad (a.6)$$

$$\sim\{\exp[-i(\mathbf{k}_u+\mathbf{K})\cdot\mathbf{t}_A]-\exp[-i(\mathbf{k}_u+\mathbf{K})\cdot\mathbf{t}_B]\} \times\int\int_{-\infty}^{\infty}\exp[-i(\mathbf{k}_u+\mathbf{K})\cdot\mathbf{r}]f(\mathbf{r})dxdy. \quad (a.7)$$

We choose the origin of the coordinate system to be at the midpoint of the line A_0B_0 (see Fig. 3) and set

$$S=l_1-l_2+1; \quad (a.8)$$

then,

$$(\mathbf{k}_u+\mathbf{K})\cdot\mathbf{t}_A=-\tfrac{1}{3}\pi S, \quad (a.9)$$

and

$$c(\mathbf{k}_u+\mathbf{K}, z)\sim\sin\tfrac{1}{3}\pi S\eta(|\mathbf{k}_u+\mathbf{K}|, z), \quad (a.10)$$

where

$$\eta(|\mathbf{k}_u+\mathbf{K}|, z)=\int\int\exp[-i(\mathbf{k}_u+\mathbf{K})\cdot\mathbf{r}]f(r)dxdy. \quad (a.11)$$

The function η is independent of direction of $\mathbf{k}_u+\mathbf{K}$ since $f(r)$ has cylindrical symmetry about the z axis. The coefficients $c(\mathbf{k}_u+\mathbf{K}, z)$ are odd in z and in $(\mathbf{k}_u+\mathbf{K})_x$. One has, then,

$$p_0=\frac{\hbar}{J}\sum_{l_1=-\infty}^{\infty}\sum_{S=1}^{\infty}\sin^2(\tfrac{1}{3}\pi S)(k_{uy}+K_y) \times\int_0^{\infty}[\eta(k_u+\mathbf{K}, z)]^2dz, \quad (a.12)$$

where J is a normalized constant,

$$J=\sum_{l_1=-\infty}^{\infty}\sum_{S=1}^{\infty}\sin^2(\tfrac{1}{3}\pi S)\int_0^{\infty}[\eta(\mathbf{k}_u+\mathbf{K}, z)]^2dz. \quad (a.13)$$

We let $f(r)$ be hydrogenic in form

$$f(r)=Ze^{-Zr/2a_0}, \quad (a.14)$$

where a_0 is the Bohr radius and Z is the effective nuclear charge. The integration indicated for η can be carried out in closed form and leads to

$$\eta(k,z)\sim\beta^{-4}[\beta z+(\beta z)^2]e^{-\beta z}, \quad (a.15)$$

with

$$\beta=[k_x^2+k_y^2+(Z/2a)^2]^{\frac{1}{2}}.$$

However,

$$\int_0^{\infty}[\eta(k,z)]^2dz\sim\beta^{-9}. \quad (a.16)$$

By substituting (a.15) into (a.12) and (a.13), one can evaluate p_0.

We use the value

$$Z/2a=1.59\ (\text{Bohr radius})^{-1},$$

as obtained by Zener[16] in a Hartree approximation to atomic carbon wave functions. With this value, the series in (a.12) and (a.13) converge rapidly. Replacing each series by the sum of the five largest terms, we find

$$p_0/\hbar=0.63\ \text{A}^{-1}. \quad (a.17)$$

[16] C. Zener, Phys. Rev. **36**, 51 (1930).